CHAPTER 25

Modelling of Wave–Current Boundary Layer in the Coastal Zone

Leszek M. Kaczmarek & Rafał Ostrowski [1]

Abstract

A 2–D numerical model of bottom turbulent boundary layer is described. The nonlinear effects associated with wave asymmetry and the nonlinear interaction of waves and currents are taken into account. The model provides a relatively simple procedure for determination of both instantaneous and time–averaged quantities of velocity and friction inside the boundary layer.

1 Introduction

The interaction of current and nonlinear waves is characteristic for a coastal zone behind and ahead of surf line because of the balance of wave asymmetry and effects bound with time–averaged current, called a return flow. Inter alia, it is possible that a time–averaged flow is offshore in the entire outer region while in the boundary layer, due to wave asymmetry, onshore flow occurs.

The problem of interaction of waves and currents will be dealt with in two regions: in a potential oscillatory flow with superimposed current and in a boundary layer, with the continuity laws satisfied at the interface of the two regions. The solution in the boundary layer is conditioned by the knowledge of the flow in the outer region.

The model takes into account nonlinear effects (i.e. wave asymmetry and those due to $\overline{Uw_\infty}$). Two steps have been proposed:

- Step I — an iterative scheme providing the slip velocity, with $\overline{Uw_\infty}$ term due to energy dissipation in the boundary layer
- Step II — a procedure yielding instantaneous and time–averaged velocity distributions in the boundary layer due to wave asymmetry.

[1]Ph. D. & M. Sc. Polish Academy of Sciences' Institute of Hydro-Engineering, IBW PAN, 7 Kościerska, 80-953 Gdańsk, Poland

2 Wave nonlinearity

2.1 Wave input asymmetry

Within nonlinear approximation the equation of motion in boundary layer has the form:

$$\frac{\partial u}{\partial t} + u\frac{\partial u}{\partial x} = \frac{\partial U}{\partial t} + U\frac{\partial U}{\partial x} + \frac{\partial}{\partial z}\left(\nu_t \frac{\partial u}{\partial z}\right) \tag{1}$$

where $u(z,t)$ i $U(t)$ are the velocities inside and at the upper limit of boundary layer, respectively.

Assuming that the velocity u does not depend on a variable x, one may neglect the convective terms and simultaneously take the nonlinearity into account by expressing the velocities of bottom oscillations $U(t)$ in potential motion by nonlinear Stokes approximation. In this way the *asymmetry* of wave with respect to still water level, defined according to the order of nonlinear approximation, is considered.

The linearized equation of motion (Eq. 1) in boundary layer reads:

$$\frac{\partial}{\partial t}(u - U) = \frac{1}{\rho}\frac{\partial \tau}{\partial z} \tag{2}$$

where $\tau(z,t)$ is the shear stress and ρ is water density.

To define time distribution of bottom friction velocity $u_f(t)$, the assumptions of Fredsoe's model (1981) formulated for sinusoidal wave and the suggestion of Fredsoe, Andersen & Silberg (1985) concerning the possibility of adaptation of the model for nonlinear wave case have been employed.

Integrating Eq. 2 over the thickness of boundary layer δ and assuming the logarithmic distribution of velocity one obtains the following differential equation:

$$\frac{dz_1}{d(\omega t)} = \frac{30\kappa^2 U(\omega t)}{k_s \omega e^{z_1}(z_1 - 1) + 1} - \frac{z_1(e^{z_1} - z_1 - 1)}{e^{z_1}(z_1 - 1) + 1}\frac{1}{U}\frac{dU}{d(\omega t)} \tag{3}$$

in which:

$$z_1 = \frac{U\kappa}{u_f} \tag{4}$$

and:

$$\delta = \frac{k_s}{30}(e^{z_1} - 1) \tag{5}$$

where k_s is Nikuradse roughness parameter and $k_s/30$ is the theoretical bed level above $z = 0$.

It is necessary to point out that the solution of Eq. 3 bases on an assumption that the boundary layer develops anew every time the flow reverses. This implies the neglect of memory effects.

As a result of numerical solution of Eq. 3, the function $z_1(t)$ is obtained and the temporal distributions of friction velocity $u_f(t)$ and boundary layer thickness $\delta(t)$ can be calculated thereafter on the basis of Equations 4 and 5.

The asymmetry of bottom velocity oscillations $U(t)$ brings about non–uniform growth of boundary layer thickness in crest and trough phases, thus non–uniform friction.

The presented computational procedure permits the determination of the characteristics of bottom friction (δ and u_f) practically for any input $U(t)$.

Making use of the definition of friction velocity:

$$u_f = \sqrt{\frac{\tau}{\rho}} \tag{6}$$

one may determine the mean shear stress within wave period T:

$$\tau_c = \frac{1}{T}\int_0^T \rho \mid u_f(t) \mid u_f(t)dt \tag{7}$$

and the corresponding mean friction velocity:

$$u_{fc} = \sqrt{\frac{\tau_c}{\rho}} \tag{8}$$

On the basis of computations one finds out that the mean friction velocity for an arbitrary nonlinear input is a positive value although the resultant water velocity at the top of the boundary layer is zero. In the computations carried out for a typical nonlinear wave in small scale laboratory tests, represented by 2nd or 3rd Stokes approximation, the quantity u_{fc}^2 has represented about 5% of the maximum shear stress u_{fmax}^2, where $u_{fmax} = max[u_f(t)]$.

The non–zero mean shear stress reflects the existence of a certain resultant current inside boundary layer, directed accordingly to wave propagation.

All earlier attempts of *theoretical* description of the resultant current induced inside a boundary layer have led to the identification of wave–induced mass flux caused by the displacement in a boundary layer. The flux arises because a phase shift exists between the horizontal and vertical flow velocities at the top of the boundary layer in non–uniform water waves. This effect will be discussed in the next section.

2.2 Discussion of vertical momentum transfer induced by the energy dissipated in a wave boundary layer

The non–zero vertical velocity w in the boundary layer results from continuity equation in the solution of Longuet–Higgins (1953) for the laminar boundary layer. The existence of this velocity indicates that an additional mean (over wave period) shear stress $\overline{uw}$ is generated inside the boundary layer. This stress attains the maximum value at the upper limit of the layer. It causes the disturbances in the region of potential flow, because there is no vertical momentum exchange represented by the term $\overline{uw}$ in linear wave motion. The approach of Longuet–Higgins implies that the form of vertical velocity w induced by the vorticity depends on the linear solution of the equation of motion. Moreover, it can be easily shown that the shear stress induced outside the boundary layer is oriented in the direction of wave propagation and the velocity is smaller by one order of magnitude than its linear counterpart.

In the case of turbulent motion, the determination of the additional shear stress generated inside the boundary layer requires, as in laminar motion, the knowledge of the linear solution of Eq. 2. This solution depends on the distribution of eddy viscosity ν_t.

Using the continuity equation and assuming:

$$\frac{\partial}{\partial x} = -\frac{1}{c}\frac{\partial}{\partial t} \tag{9}$$

where c is a phase velocity of wave, one may determine the additional vertical velocity w_∞ outside the boundary layer:

$$w_\infty = -\frac{\partial}{\partial x}\int_{\frac{k_s}{30}}^{\frac{k_s}{30}+\delta}(u-U)dz = \frac{1}{c}\int_{\frac{k_s}{30}}^{\frac{k_s}{30}+\delta}\frac{\partial}{\partial t}(u-U)dz \tag{10}$$

After taking into account Eq. 2 integrated over the boundary layer thickness, Eq. 10 transforms into the form:

$$w_\infty = -\frac{\tau_0}{c\rho} = -\frac{u_f \mid u_f \mid}{c} \tag{11}$$

The considerations of Deigaard & Fredsoe (1989) reveal that the nonlinearities bound with the generation of an additional vertical velocity w_∞ at the top of boundary layer i.e. the nonlinearities linked with the terms $\overline{UW}$ are closely associated with the dissipation of wave energy. If the energy dissipation is neglected one may skip the additional stresses generated at the top of the boundary layer (the current induced by these stresses does not exist).

Finally it is worthwhile pointing out that the stress $\overline{uw_\infty}$ equals zero at the bottom and reaches the maximum value at the top of boundary layer while the effects of wave asymmetry play the key role very close to the bottom.

The above conclusions will be helpful for formulation of a model in Section 3.

3 Wave and current interaction

Integrating Eq. 2 over the thickness of boundary layer in the similar manner as in Section 2.1 and assuming $\tau(\delta) = -\rho u_{f0}^2$ and $\tau_0 = \rho|u_f|u_f$, cf. Fredsoe (1984), one obtains the following differential equation:

$$\frac{dz_1}{d(\omega t)} = \frac{30z_1^2\left[\left|\frac{\kappa U}{z_1} - u_{f0}\right|\left(\frac{\kappa U}{z} - u_{f0}\right) + u_{f0}^2\right]}{\omega k_s U[e^{z_1}(z_1-1)+1]} - \frac{z_1(e^{z_1}-z_1-1)}{e^{z_1}(z_1-1)+1}\frac{1}{U}\frac{dU}{d(\omega t)} \tag{12}$$

in which:

$$z_1 = \frac{\kappa U}{u_f + u_{f0}} \tag{13}$$

and:

$$\delta = \frac{k_s}{30}(e^{z_1}-1) \tag{14}$$

In Equation 12 the *nonlinear wave input* $U(t)$ can be involved, given by any Stokes approximation (for instance of 2nd or 3rd order). Both the current friction velocity u_{f0} and the variable z_1 are unknown. Therefore the use of iteration method in the first stage of solution is proposed.

Introducing the defect velocity $u_d(z,t) = u(z,t) - U(t)$ one has the equation of motion (Eq. 2) in the form:

$$\frac{\partial u_d}{\partial t} = \frac{\partial}{\partial z}\left(\nu_t \frac{\partial u_d}{\partial z}\right) \tag{15}$$

The following approximate initial condition is assumed:

$$u_d(z, t_0) = 0 \tag{16}$$

and the boundary conditions are:

$$u_d(\frac{k_s}{30}, \omega t) = -U(\omega t) \tag{17}$$

$$u_d(2\delta_m + \frac{k_s}{30}, \omega t) = 0 \tag{18}$$

Eq. 15 is solved numerically by an implicit method involving the Crank – Nicholson scheme. Because the approximate initial condition (Eq. 16) has been assumed, the computations have had to cover the time corresponding to a few wave periods until the compatibility between $u_d(z, t_0 + N \cdot T)$ and $u_d[z, t_0 + (N+1) \cdot T]$ is reached. The number of required runs N depends on wave parameters and is three to five.

Within the first stage of the solution, an interaction of a *sinusoidal* wave and the steady current is considered. A simple iterative procedure presented by Kaczmarek & Ostrowski (1991) ensures the determination of the current friction velocity u_{f0} by matching the mean shear stress at the top of boundary layer. Mean velocities are also matched at the upper limit of boundary layer: the slip velocity calculated from equations governing in the outer region and the mean velocity at the top of boundary layer (see Appendix).

Within the second stage of the solution, the temporal distribution of total friction velocity u_f is determined on the basis of Eq. 12 for the quantity u_{f0} computed previously and for nonlinear oscillatory input $U(t)$.

As a result of numerical solution of Eq. 12, the function $z_1(\omega t)$ is obtained and the temporal distributions of friction velocity $u_f(\omega t)$ and boundary layer thickness $\delta(\omega t)$ are determined from Eqs. 13 and 14, respectively. Then one can easily calculate the root mean square friction velocity u_{fc} from Eqs. 7 and 8.

The following distribution of eddy viscosity ν_t is assumed:

$$\begin{aligned} \nu_t(z) &= \kappa \hat{u}_f z && \text{for} \quad \tfrac{k_s}{30} \le z \le \tfrac{\delta_m}{4} + \tfrac{k_s}{30} \\ \nu_t(z) &= \kappa \hat{u}_f \left(\tfrac{\delta_m}{4} + \tfrac{k_s}{30}\right) && \text{for} \quad z > \tfrac{\delta_m}{4} + \tfrac{k_s}{30} \end{aligned} \tag{19}$$

Let us notice that the above distribution is based on the friction velocity $\hat{u}_f$, which couples the effects of a current and wave asymmetry (determined within the two–stage approach). The equivalent friction velocity $\hat{u}_f$ has been assumed as:

$$\hat{u}_f = \max\left(|u_f(\omega t)|\right) \tag{20}$$

while the mean boundary layer thickness the authors propose to determine as:

$$\delta_m = \max(\delta_1, \delta_2) \tag{21}$$

where δ_1 and δ_2 are the boundary layer thicknesses at the moments corresponding to maximum and minimum total (oscillatory and current) input $U(t) + V$, respectively.

The equation of motion for the case of linear wave and current may be solved separately with separate boundary conditions. As it was pointed out by Kaczmarek & Ostrowski (1991), the assumption of time-independence of eddy viscosity ν_t in the boundary layer allows one to treat the combined wave and current motion by separate equations. The effect of nonlinear interaction between waves and a current is incorporated in the eddy viscosity, thus modelling of the turbulent viscosity ν_t.

Hence the determination of intantaneous velocities $u(z,t)$ may be the sum of the solution of equation of motion for wave only with the oscillatory velocity at the top of boundary layer as a boundary condition and the current described by equations:

$$\kappa \hat{u}_f z \frac{\partial u_c}{\partial z} = u_{fc}|u_{fc}| \tag{22}$$

in the range $< k_s/30; \delta_m/4 + k_s/30 >$ and

$$\kappa \hat{u}_f \left(\frac{\delta_m}{4} + \frac{k_s}{30} \right) \frac{\partial u_c}{\partial z} = u_{fc}|u_{fc}| \tag{23}$$

in the range $(\delta_m/4 + k_s/30; \delta_m/2 + k_s/30 >$.

The friction velocity $u_f(\omega t)$, the boundary layer thickness $\delta(\omega t)$ and the root time-mean square friction velocity u_{fc} are determined from the solution of Equation 12.

Integrating Eqs. 22, 23 and taking advantage of the condition $u_c(z = k_s/30) = 0$ and the condition of continuity of u_c at $z = \delta_m/4 + k_s/30$ one comes up with the formulas:

$$u_c(z) = \frac{u_{fc}|u_{fc}|}{\kappa \hat{u}_f} ln \frac{z}{\frac{k_s}{30}} \tag{24}$$

in the range $< k_s/30; \delta_m/4 + k_s/30 >$ and

$$u_c(z) = \frac{u_{fc}|u_{fc}|}{\kappa \hat{u}_f \left(\frac{\delta_m}{4} + \frac{k_s}{30} \right)} \left(z - \frac{\delta_m}{4} - \frac{k_s}{30} \right) + \frac{u_{fc}|u_{fc}|}{\kappa \hat{u}_f} ln \frac{\frac{\delta_m}{4} + \frac{k_s}{30}}{\frac{k_s}{30}} \tag{25}$$

in the range $(\delta_m/4 + k_s/30; \delta_m/2 + k_s/30 >$.

The nonlinear wave on a steady current is the most interesting case from a practical point of view, as the resultant shear stress direction controls the direction of the resultant flow in the combined boundary layer. Therefore the quantity u_{fc} is of a great importance: if it is positive, the effects of wave asymmetry will prevail and the mean flow in the wave-current boundary layer will be directed shorewards; if u_{fc} is negative, the steady current will prevail, and the resultant flow in the boundary layer will be directed seawards. For both situations the mean velocity profile can be calculated from of Eq. 24 in the range $< k_s/30; \delta_m/4 + k_s/30 >$

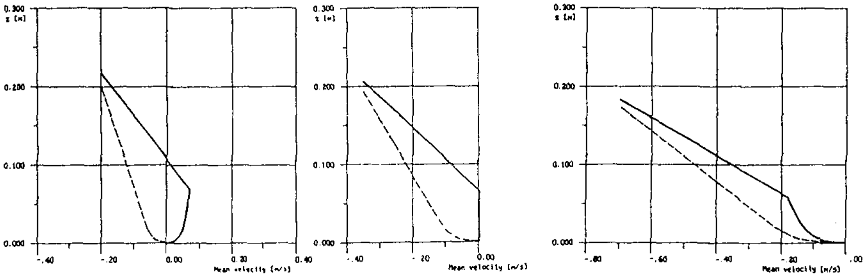

Fig. 1. Mean current velocity distributions in boundary layer as a result of interaction between nonlinear (solid line) or sinusoidal (dashed line) waves and a current

and Eq. 25 in the range $(\delta_m/4 + k_s/30; \delta_m/2 + k_s/30 >$ as in the case of nonlinear wave and current interaction the shear stress is assumed as constant in the range $< k_s/30; \delta_m/2 + k_s/30 >$. The choice of the upper limit where the shear stress is constant is rather arbitrary but it follows an assumption made with respect to wave boundary layer. The authors have proposed the upper limit of this region as the ordinate corresponding to the level at which the maximum (or minimum) velocity profile reaches the free stream velocity. In accordance with Jonsson & Carlsen (1976) $\delta_m/2 + k_s/30$ is the most consistent measure. In the range $(\delta_m/2 + k_s/30; 2\delta_m + k_s/30 >$ the mean velocity profile is assumed to change linearly upwards and to attain the value of slip velocity at the top of boundary layer. To analyse and distinguish the two major types of waves propagating against a current, sample computations have been carried out for the wave parameters corresponding to the laboratory experiment by Jonsson & Carlsen (1976): $h = 10$ m, $H = 5.3$ m, $T = 8.39$ s. The wave has been approximated by Stokes theory of 2nd order. Additionally three currents of different slip velocities have been assumed: $V = 0.20$ m/s, $V = 0.35$ m/s and $V = 0.70$ m/s. The resultant mean velocity distributions (solid line) in comparison with the profiles obtained for sinusoidal wave and current interaction (dashed line) are depicted in Fig. 1.

Having solved the equation of motion in boundary layer (Eq. 15) one may superimpose the instantaneous velocity profiles on the mean current distribution given by Eqs. 24 and 25 in the range $< k_s/30; \delta_m/2 + k_s/30 >$. In the range $(\delta_m/2 + k_s/30; 2\delta_m + k_s/30 >$ the mean velocity profile changes linearly upwards and attains the value of slip velocity at the top of boundary layer. This mean current velocity is also superimposed on the instantaneous velocity distributions.

4 Comparison between theory and measurements

4.1 Velocity in wave–current bottom boundary layer

Results of computations have been compared with the laboratory measurements by Hwung & Lin (1990). The experiments were carried out in a 9.5×0.7×0.3 m wave tank in which the bottom was adjusted on one–fifteenth slope. The velocities

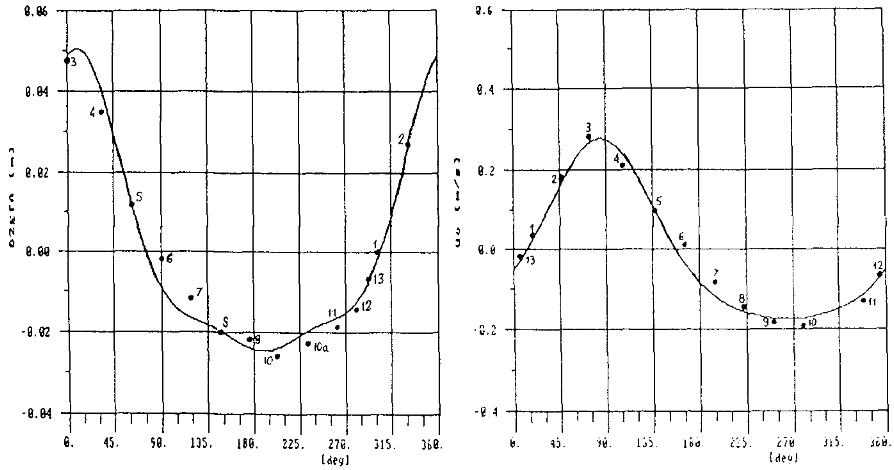

Fig. 2. Measured (•) and calculated (–) water surface elevation (left) and wave input (right)

of water were measured in 13 testing sections (including the boundary layer) situated along the flume. The comparison of computated data and measurements concern *Case 2* of experimental wave parameters: initial depth $h = 0.33$ m, initial wave height $H = 6.6$ cm, wave period $T = 1.23$ s.

Although it is possible to provide a complex solution in the outer region using one of the models dealing with return flow and in the boundary layer using the present approach, it is well worth focusing attention on the precision of solution in the boundary layer, being a major topic of the paper. Therefore the value of the slip velocity V has been taken from the measurements of Hwung & Lin (1990) to obtain the best fit of the boundary condition at the upper limit of boundary layer.

The computed and measured instantaneuos velocity profiles have been compared for the testing section $P4$. The water surface elevation $\zeta(\omega t)$ and the wave input $U(\omega t)$ have been determined by the theory of Borgman and Chappelear (Stokes approximation of 3rd order), Fig. 2. The assumed time distributions of $\zeta(\omega t)$ and $U(\omega t)$ have been a little bit shifted to obtain the best fit with respect to the recorded ones.

The instantaneous and mean velocity profiles have been computed using the procedure presented in the previous section. The parameter of equivalent roughness k_s has been estimated as 2 mm. The instantaneous velocities are given in Fig. 3. The agreement of computed and measured instantaneous velocity profiles is satisfactory, especially at the moments corresponding to the best fit between recorded and assumed wave inputs $U(\omega t)$.

The calculated mean velocity profiles for the testing sections $P1$, $P3$, $P4$ and $P6$ are given in Fig. 4. In general, they all correspond to the measured ones very

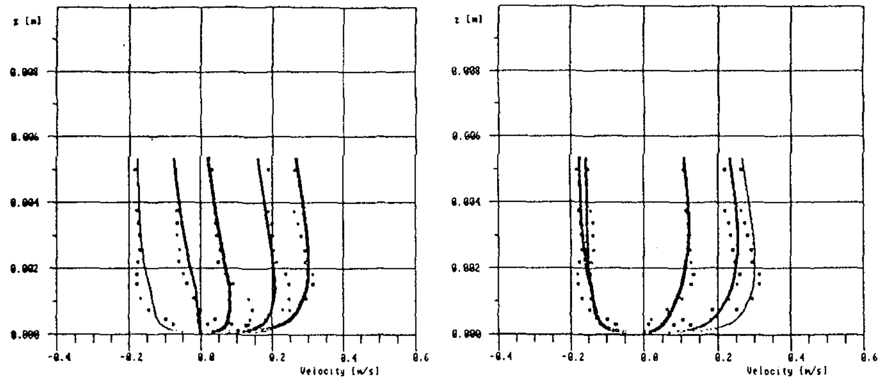

Fig. 3. Measured (•) and computed (–) instantaneous velocity distributions

well. As the testing section $P1$ lies in the range of application of Stokes 2nd order theory, the velocity has also been determined with this approximation (dashed line).

4.2 Undertow combined with a bottom boundary layer

The case of the wave propagating perpendicularly to the shoreline is considered. The oscillatory motion is accompanied by the undertow which compensates the mass flux carried shoreward by the breaking waves. The eddy viscosity model (Eqs. 19) in the bottom boundary layer is assumed. The eddy viscosity ν_{tc} in outer region is assumed vertically constant. As shown by Svendsen (1984) the inclusion of a conceptually realistic depth–variation of ν_{tc} has the effects of secondary importance when compared to the effects of incorporating alternative boundary conditions at the bottom.

The vertical distribution of the mean current velocity in the outer region $U_c(z)$ may be estimated by the following formula, cf. Svendsen (1984):

$$U_c(z) = \frac{1}{2}\,\alpha(z+h)^2 + \left(2\,\frac{U_m - V}{d_{tr}} - \frac{1}{3}\,\alpha\,d_{tr}\right)\,(z+h) + V \tag{26}$$

in which

$$\alpha = \frac{\alpha_1(x)}{\nu_{tc}} \tag{27}$$

$$\alpha_1(x) = \frac{\partial}{\partial x}\left(\overline{u_w^2} + g\bar{\eta}\right) \tag{28}$$

where U_m is the total mean mass flux below the wave trough, d_{tr} is the distance between sea bottom and wave trough, $\overline{u_w^2}$ is mean square oscillatory horizontal velocity, $\bar{\eta}$ is the set-up and g is the acceleration of gravity. The coordinate system begins at mean water level in this case and z axis is directed upwards.

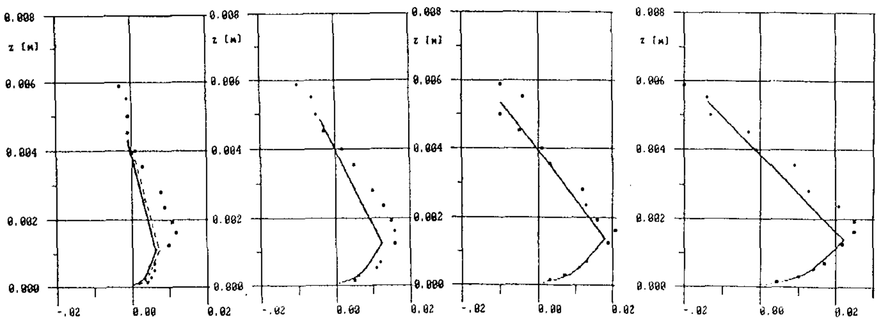

Fig. 4. Measured (•) and computed (–) mean velocity profiles at testing sections $P1$, $P3$, $P4$, $P6$

The derivative of Eq. 26 reads:

$$\frac{\partial U_c(z)}{\partial z} = \alpha\ (z+h) + \left(2\ \frac{U_m - V}{d_{tr}} - \frac{1}{3}\ \alpha\ d_{tr}\right) \tag{29}$$

The shear stress at the lower limit of the undertow region is given by the formula:

$$\tau_e = \rho \nu_{tc}\ \left.\frac{\partial U_c(z)}{\partial z}\right|_{z=-h} \tag{30}$$

Basically, the slip velocity V which corrensponds to the one at the top of the boundary layer is unknown and that is the reason of iteration in our solution of the problem. The quantity V must match the mean velocity at the top of boundary layer as well as τ_e must be equal to the mean shear stress at the top of boundary layer calculated on the basis of instantaneous velocity profiles from Eq. 15.

The comparisons between the measurements of Stive & Wind and Hansen & Svendsen experiments (Stive & Wind 1986) and the results obtained with the use of proposed method are shown in Figs. 5 and 6.

As it is seen the slip velocity obtained with the use of presented procedure does not differ much from that which would exist if an assumption was made of $\tau_e(z = -h)$ equal zero. This confirms experimental observations of Stive & Wind (1986). The above conclusion is of great importance for calculating the undertow velocity distribution in practical use. Thus assuming $\partial U_c(z)/\partial z|_{z=-h} = 0$ in Eq. 29 one obtains the simplified formula for slip velocity:

$$V = U_m - \frac{1}{6}\ \alpha\ d_{tr}^2 \tag{31}$$

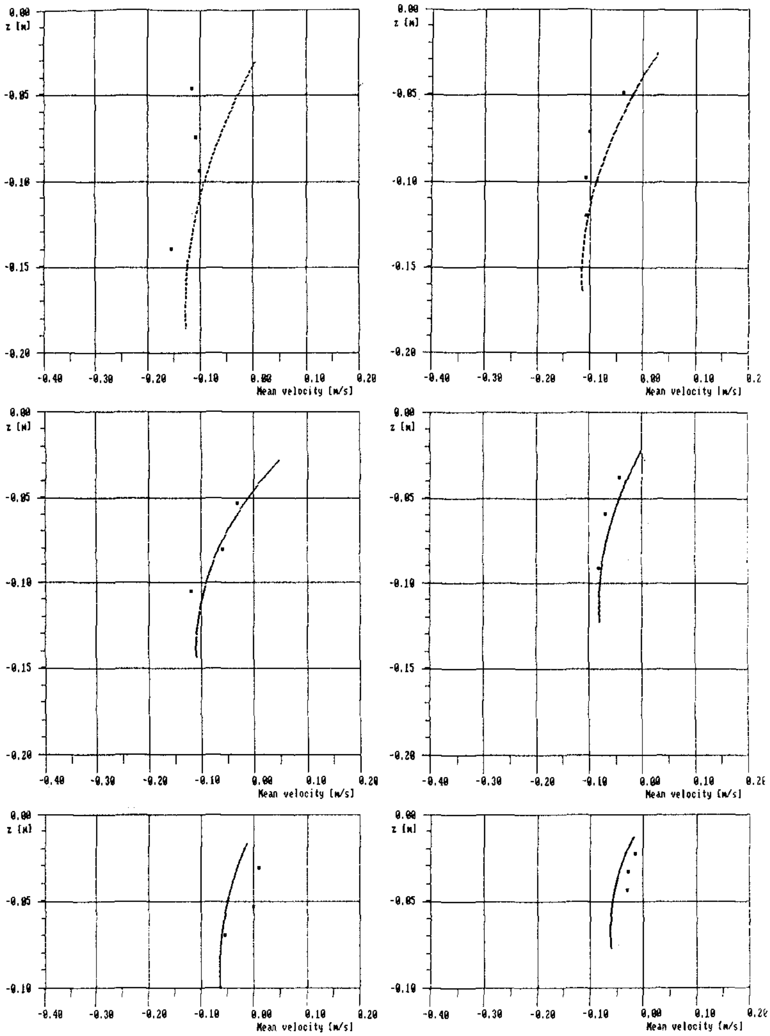

Fig. 5. Measured and calculated undertow; tests by Stive & Wind (1986)

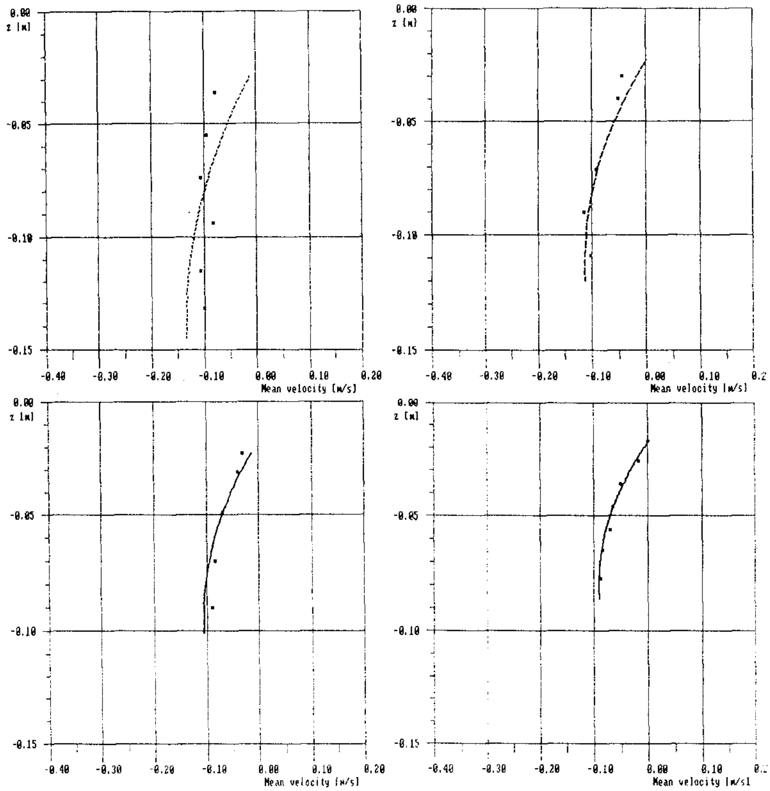

Fig. 6. Measured and calculated undertow; tests by Hansen & Svendsen (Svendsen 1984)

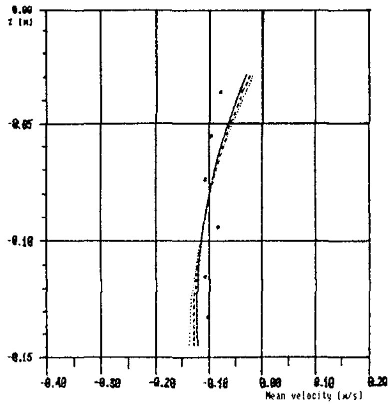

Fig. 7. The $\overline{Uw_\infty}$ contribution to undertow profile

In the computations k_s was assumed as 1 mm for all sets of data after Svendsen & Hansen (1988).

It is worthwhile remembering that the $\overline{UW}$ term originating from the organized orbital motion vanishes at the top of boundary layer, while the $\overline{Uw_\infty}$ associated with the energy dissipated in a wave boundary layer possesses a certain value, cf. the discussion in section 2.2. It is interesting to evaluate the contribution of this term to the undertow distribution near the bottom. To this end the $\overline{Uw_\infty}$ term has been estimated from Eq. 11 and incorporated in the iterative scheme by superposition with the undertow shear stress at the top of boundary layer. The effect of $\overline{Uw_\infty}$ on the undertow distribution has been evaluated for one of the cases of Hansen & Svendsen's (1984) experiment and is depicted in Fig. 7 (solid line) in comparison with the undertow profile without this effect (dashed line). Additionally, the undertow distribution computed with the assumption of zero undertow shear stress at the top of boundary layer is given (dotted line). As one could have expected, the contribution of $\overline{Uw_\infty}$ is very small and the proposed formula for slip velocity (Eq. 31) obtained with the assumption of zero undertow shear stress at the bottom is sufficient for practical engineering purposes.

5 Conclusions

The theoretical model describing both instantaneous and time-averaged quantities of velocity and friction inside the turbulent boundary layer generated by the interaction of nonlinear wave and current has been presented. The treatment of the paper is restricted to the two-dimensional flow, in which the intersection angle between the direction of wave propagation and that of the steady current is either 0^o or 180^o. The model takes into account nonlinear effects, i.e. wave asymmetry and the effects associated with $\overline{Uw_\infty}$.

The results of computations of velocities inside the boundary layer under nonlinear wave and current have been compared with the laboratory data of Hwung

& Lin's (1990) experiment. The agreement of computed and measured, both instantaneous and mean, velocity profiles is satisfactory.

The effect of $\overline{Uw_{\infty}}$ (associated with energy dissipation in the wave boundary layer) on the undertow distribution has been evaluated for one of the cases of Hansen & Svendsen's (1984) experiment. The contribution of this term has been found out to be very small. This implies that the proposed formula for slip velocity obtained with the assumption of zero undertow shear stress at the bottom is sufficient for practical engineering purposes.

Appendix: Iterative scheme for undertow and bottom boundary layer

1. Assumption of V
2. Assumption of u_{f0}
3. Computation of u_{fc} (Eqs. 12, 13, 7, 8) and τ_e (Eq. 30)
4. Verification whether $\tau_e = \rho u_{fc}^2$

5a. IF NOT: correction of u_{f0} and GO TO item 3
5b. IF YES: computation of $u_c(z)$
6. Verification whether $V = u_c(2\delta_m + k_s/30)$
7a. IF NOT: correction of V and GO TO item 2
7b. IF YES: END

Acknowledgements
The study has been sponsored by KBN and PAN, Poland, under programme 2 IBW PAN, which is hereby gratefully acknowledged. The Authors wish to thank Prof. R. Zeidler for the discussions and helpful suggestions throughout the study.

References

Deigaard R., Fredsoe J. (1989), Shear stress distribution in dissipative water waves, Coastal Engng. 13, 357–378
Fredsoe J. (1981), A simple model for the wave boundary layer, *Prog. Rep. 54*, Inst. Hydrodyn. and Hydraulic Engng. Tech. Univ. Denmark
Fredsoe J. (1984), Turbulent boundary layer in wave–current motion, *J. Hydraulic Engng.*, ASCE, Vol. 110, No 8
Fredsoe J., Andersen O.H., Silberg S. (1985), Distribution of suspended sediment in large waves, *J. Wtrway., Port, Coast. and Oc. Engng.*, ASCE, Vol. 111, No 6
Hansen J. Buhr, Svendsen I.A. (1984), A theoretical description and experimental study of undertow, *Proc. 19th Int. Conf. on Coastal Engng.*, Houston
Hwung H.H., Lin C. (1990), The mass transport of waves propagating on a sloping bottom, *Proc. 22nd Coast. Engng. Conf.*, Delft
Jonsson I.G., Carlsen N.A. (1976), Experimental and theoretical investigations in an oscillatory turbulent boundary layer, *J. Hydr. Res.*, Vol. 14, No 1
Kaczmarek L.M., Ostrowski R. (1991), Modelling of wave–current boundary layers with application to surf zone, *Hydrotechnical Archives*, Vol. XXXIX, No 1–2
Longuet–Higgins M.S. (1953), Mass transport in water waves, *Philos. Trans. R. Soc. London*, Ser. A, 245: 535–581
Stive M.J.F., Wind H.G. (1986), Cross–shore mean flow in the surf zone, *Coastal Engng. 10*, 325–340
Svendsen I.A. (1984), Mass flux and undertow in a surf zone, *Coastal Engng. 8*, 347–365
Svendsen I. A., Hansen J. Buhr (1988), Cross–shore currents in surf–zone modelling, Coast. Engng., Vol. 12, No 1